OPEN ACCESS
Freely Available Online

JOURNAL OF ADVANCED PHARMACEUTICAL SCIENCE AND TECHNOLOGY
ISSN NO: 2328-0182

Research article

DOI: 10.14302/issn.2328-0182.japst-21-3772

Characterization of the Consciousness Energy Healing Treated Cholecalciferol Using LC-MS and GC-MS Spectrometry

Dahryn Trivedi[1], Mahendra Kumar Trivedi[1], Alice Branton[1], Snehasis Jana[2,*]

[1]Trivedi Global, Inc., Henderson, USA
[2]Trivedi Science Research Laboratory Pvt. Ltd., Thane (W), India

Abstract

Vitamin D_3 (cholecalciferol) is a fat-soluble vitamin, which widely used for the prevention and treatment rickets, osteoporosis, arthritis, Parkinson's and Alzheimer's diseases, autoimmune disease, dementia, glucose intolerance, etc. The impact of the Trivedi Effect®-Consciousness Energy Healing Treatment on the structural properties and the isotopic abundance ratio of cholecalciferol were evaluated using LC-MS and GC-MS spectroscopy. The test sample cholecalciferol was divided into control and treated parts. Only, the treated cholecalciferol was received the Trivedi Effect®-Consciousness Energy Healing Treatment remotely by a renowned Biofield Energy Healer, Dahryn Trivedi. The LC-MS spectra of both the samples at retention time (R_t) ~22 minutes exhibited the mass of the molecular ion peak at *m/z* 385.25 (calcd for $C_{27}H_{45}O^+$, 385.35). The LC-MS based isotopic abundance ratio of P_{M+1}/P_M in the treated cholecalciferol was increased by 0.74% compared with the control sample. But, the GC-MS based isotopic abundance ratio of P_{M+1}/P_M and P_{M+2}/P_M in the treated cholecalciferol was significantly increased by 66.39% and 62.69%, respectively compared with the control sample. Hence, ^{13}C, ^{2}H, ^{17}O, and ^{18}O contributions from $C_{27}H_{44}O^+$ to *m/z* 386 and 387 in the treated cholecalciferol were significantly increased compared with the control sample. The isotopic abundance ratios of P_{M+1}/P_M ($^{2}H/^{1}H$ or $^{13}C/^{12}C$ or $^{17}O/^{16}O$) and P_{M+2}/P_M ($^{18}O/^{16}O$) in the treated cholecalciferol were significantly increased as compared to the control sample. The increased isotopic composition of the Trivedi Effect®-Consciousness Energy Healing Treated cholecalciferol might have altered the neutron to proton ratio in the nucleus *via* the possible mediation of neutrino. The increased isotopic abundance ratio of the treated cholecalciferol may increase the intra-atomic bond strength, increase its stability. The new form of cholecalciferol would be better designing novel pharmaceutical formulations that might be more stable and more efficacious for the prevention and treatment of various diseases such as vitamin D deficiency, rickets, osteoporosis, arthritis, multiple sclerosis, cancer, diabetes mellitus, mental disorders, cardiovascular diseases, hypertension, infections, influenza, cognitive impairment in older adults, Parkinson's and Alzheimer's diseases, autoimmune disease, dementia, glucose intolerance, multiple sclerosis, etc.

Corresponding author: Snehasis Jana, Trivedi Science Research Laboratory Pvt. Ltd., Thane (W), Maharashtra, India. Tel: +91- 022-25811234; Email: publication@trivedisrl.com

Citation: Dahryn Trivedi, Mahendra Kumar Trivedi, Alice Branton, Snehasis Jana (2021) Characterization of the Consciousness Energy Healing Treated Cholecalciferol Using LC-MS and GC-MS Spectrometry. Journal of Advanced Pharmaceutical Science And Technology - 2(4):40-50. https://doi.org/10.14302/issn.2328-0182.japst-21-3772

Keywords: Cholecalciferol, The Trivedi Effect®, Consciousness Energy Healing Treatment, Isotopic abundance

Received: Mar 09, 2021 **Accepted:** Apr 02, 2021 **Published:** Apr 15, 2021

Editor: Fatma Mohammed Mady, Department of Pharmaceutics, Minia University, Egypt.

Introduction

Vitamin D_3 (cholecalciferol) is a fat-soluble vitamin and a hormone precursor. Vitamin D_2 is found naturally in the sun-exposed mushrooms and humans synthesize vitamin D_3 in the skin on exposure to UV light from the sun [2]. Vitamin D synthesized in skin and diet is biologically inert. It gets activated by hydroxylation in the liver and kidney to 1,25-dihydroxycholecalciferol (calcitriol). Vitamin D_2 and D_3 differ chemically in their side chains. These differences in the structure alter their binding to the vitamin D binding protein (DBP) and their metabolism. DBPs are found in most of the body parts, *i.e.,* heart, lungs, kidney, brain, liver, pancreas, intestines, muscles, nervous system, gonads, etc. Vitamin D regulates the various functions of the brain, muscles, lungs, liver, kidneys, heart, pancreas, intestines, and immune system. Vitamin D receptor response elements with hundreds of genes directly or indirectly influence cell-to-cell communication, normal cell growth, cell cycling and proliferation, cell differentiation, neurotransmission, hormonal balance, increase calcium (30-40%) and phosphorus (80%) absorption, skin health, immune, and cardiovascular functions [3-5].

Children, young and middle-aged people are equally high risk for vitamin D deficiency worldwide. Inadequate exposure to sunlight, high body mass index (>30 kg/m^2), fat malabsorption syndromes and bariatric patients, patient taking anticonvulsants and anti AIDS/ HIV medications, chronic liver disease, familial hypophosphatemia, and hypocalcaemia is associated with hypoparathyroidism are the cause of the vitamin D deficiency [2, 4]. Vitamin D deficiency may cause abnormalities in calcium, phosphorus, and bone metabolism, rickets, osteoporosis, arthritis, multiple sclerosis, cancer, diabetes mellitus, mental disorders, cardiovascular diseases, hypertension, infections, influenza, cognitive impairment in older adults, Parkinson's and Alzheimer's diseases, autoimmune disease, dementia, glucose intolerance, multiple sclerosis, etc. [1, 2, 5, 6-8]. As per the literature, 15 µg/ d (600 IU per day) is required for all individuals between the ages of 1 and 70 years old [1-4]. High dose of vitamin D supplementation may cause toxicity like hypercalcemia, polyuria, polydipsia, weakness, mental retardation, and insomnia [8]. The stability of vitamin D is more concerned as it is more sensitive to heat and light [9, 10].

Vitamin D_3 bioavailability directly affected by various factors such as dietary fiber, genetic factors, age, skin colour, and status of vitamin D_3 [11]. The Trivedi Effect®-Consciousness Energy Healing Treatment is a form of Energy Therapy improved the bioavailability profile of several nutraceutical and pharmaceutical compounds, *i.e.,* resveratrol, berberine, 25-hydroxyvitamin D_3 [25(OH)D_3], etc. [12-14]. The Trivedi Effect® is a scientifically proven Energy Therapy in which a Biofield Energy Healer can harness this inherently intelligent energy from the Universe and transfer it anywhere on the planet through the possible mediation of neutrinos [15]. The Biofield-based Energy Healing Therapies nowadays has been used against various disease conditions [17, 18]. The Energy Therapy has been recognized worldwide as a Complementary and Alternative Medicine (CAM) health care approach by the National Center of Complementary and Integrative Health (NCCIH) with other therapies, medicines and practices such as aromatherapy, yoga, Qi Gong, Tai Chi, Ayurvedic medicine, traditional Chinese medicines, chiropractic/osteopathic manipulation, homeopathy, acupressure, acupuncture, hypnotherapy, movement therapy, naturopathy, Reiki, etc. [19]. Such therapies have been well accepted by most of the U.S.A. people [20]. Similarly, the Trivedi Effect®-Consciousness Energy Healing Treatment also potentially transform the characteristic properties of metals and ceramic [21-24], organic compounds [25, 26], microbes [27, 28], and improve the yield of crops [29, 30], alteration of the isotopic abundance ratio [31, 32].

Study on the natural stable isotope ratio analysis has a range of applications in several fields of sciences to understand the isotope effects resulting from the alterations of the isotopic composition [33-35]. Liquid chromatography-mass spectrometry (LC-MS) and Gas chromatography-mass spectrometry (GC-MS) is widely used for the analysis of isotope ratio with sufficient precision [34]. In this experiment, the LC-MS and GC-MS were used to characterize the structural properties and to evaluate the isotopic abundance ratio of P_{M+1}/P_M ($^2H/^1H$ or $^{13}C/^{12}C$ or

$^{17}O/^{16}O$) and P_{M+2}/P_M ($^{18}O/^{16}O$) in the Trivedi Effect®-Consciousness Energy Healing Treated cholecalciferol compared to the control sample.

Materials and Methods

Chemicals and Reagents

The test sample cholecalciferol (> 98%) was procured from Sigma-Aldrich, India. Similarly, the other chemicals used in the experiments were purchased in India.

Consciousness Energy Healing Treatment Strategies

The test sample cholecalciferol powder was divided into two parts, *i.e.,* control and treated parts. The control cholecalciferol powder sample did not receive the Trivedi Effect®-Consciousness Energy Healing Treatment. But, the control cholecalciferol was treated with a "sham" healer who did not have any understanding of the Consciousness Energy Healing Treatment. However, the treated part of cholecalciferol was received the Trivedi Effect®-Consciousness Energy Healing Treatment remotely under standard laboratory conditions for 3 minutes by the renowned Biofield Energy Healer, Dahryn Trivedi, USA. Finally, both the samples were kept in sealed conditions and characterized using modern analytical techniques.

Characterization

Liquid Chromatography-Mass Spectrometry (LC-MS) Analysis and Calculation of

Isotopic Abundance Ratio

The LC-MS analysis of the cholecalciferol samples was carried out with the help of LC-MS ThermoFisher Scientific, the USA equipped with an ion trap detector connected with a triple-stage quadrupole MS. The column used here was a reversed phase Thermo Scientific Synchronis C18 (Length-250 mm X ID 4.6 mm X 5 micron), maintained at 25°C. Methanol was used as a diluent for the sample preparation. 20 µL of cholecalciferol solution was injected, and the analyte was eluted using acetonitrile + methanol (80:20) pumped at a constant flow rate of 1.5 mL/min with the total run time of 30 min. Peaks were monitored at 300 nm using the PDA detector. The mass spectrometric analysis was performed under atmospheric pressure chemical ionization (APCI) +ve ion mode.

The values of the natural isotopic abundance (H, C, and O) of the common elements are obtained from the literature [35-38]. The LC-MS based isotopic abundance ratios (P_{M+1}/P_M) for the control and Biofield Energy Treated cholecalciferol was calculated using the equation (1).

$$\% \text{ Change in isotopic abundance ratio} = [(IAR_{Treated} - IAR_{Control})/ IAR_{Control}) \times 100] \quad (1)$$

Where $IAR_{Treated}$ is the isotopic abundance ratio of the treated sample and $IAR_{Control}$ is the isotopic abundance ratio of the control sample.

Gas Chromatography-Mass Spectrometry (GC-MS) Analysis

GC-MS of both the samples of cholecalciferol was analyzed with the help of Perkin Elmer Gas chromatograph equipped with a PE-5MS (30M x 250 micros x 0.250 microns) capillary column and coupled to a single quadrupole mass detector was operated with electron impact (EI) ionization in positive mode. The oven temperature was maintained from 150°C (5 min hold) to 280°C (17 min hold) @ 10°C /min with a total run time of 35 minutes. The sample was prepared taking 50 mg of the cholecalciferol in 2.5 ml methanol as a diluent. The GC-MS based isotopic abundance ratios (P_{M+1}/P_M and P_{M+2}/P_M) for the control and Biofield Energy Treated cholecalciferol was calculated using equation (1).

Results and Discussion

Liquid Chromatography-Mass Spectrometry (LC-MS)

The chromatograms of both the samples are shown in Figure 1. A single major chromatographic peak of the control and treated cholecalciferol was observed at retention time (R_t) of 21.5 and 21.8 minutes, respectively (Figure 1). This indicated that the polarity of both the samples was very close to each other.

The mass spectra of both the samples are shown in Figure 2. The mass spectra of both the samples corresponding to the R_t ~22 minutes exhibited the presence of the molecular ion of cholecalciferol ($C_{27}H_{45}O^+$) adduct with hydrogen ion at *m/z* 385.25 (calcd for $C_{27}H_{45}O^+$, 385.35) along with the lower mass peak $[M\text{-}OH]^+$at *m/z* 367.33 (calcd for $C_{27}H_{43}^+$, 367.3)

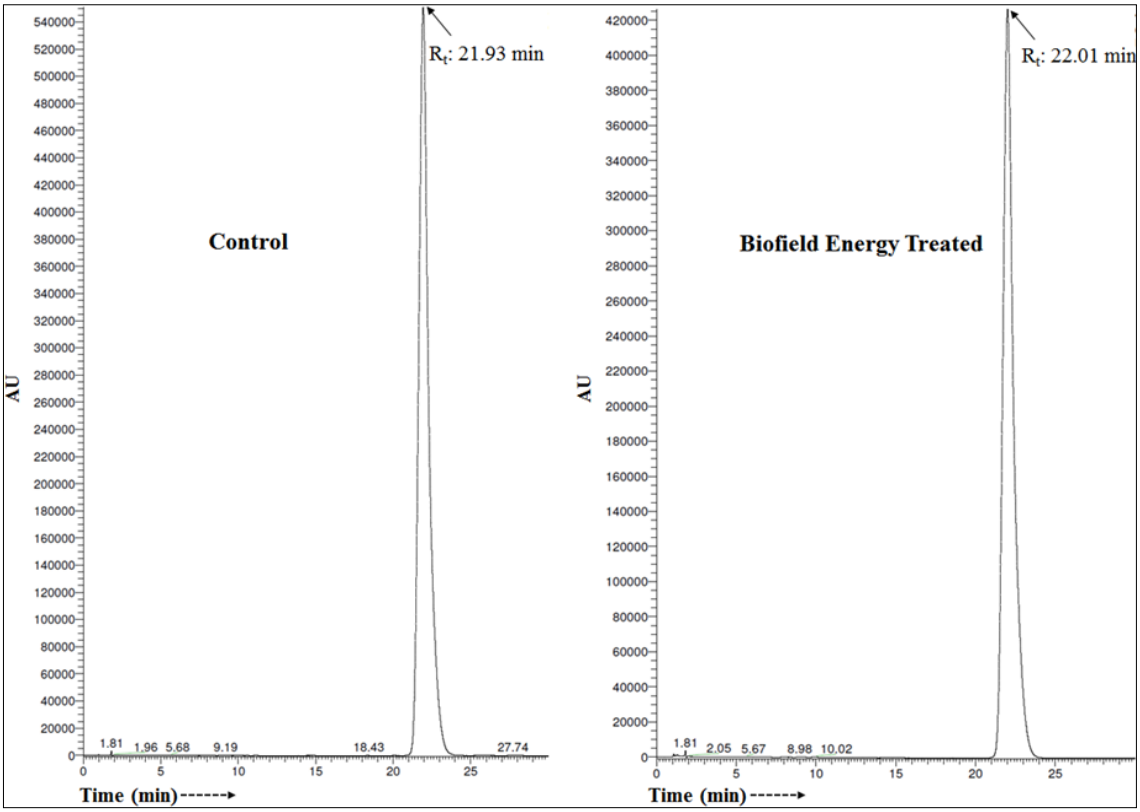

Figure 1. Liquid chromatograms of the control and Biofield Energy Treated cholecalciferol.

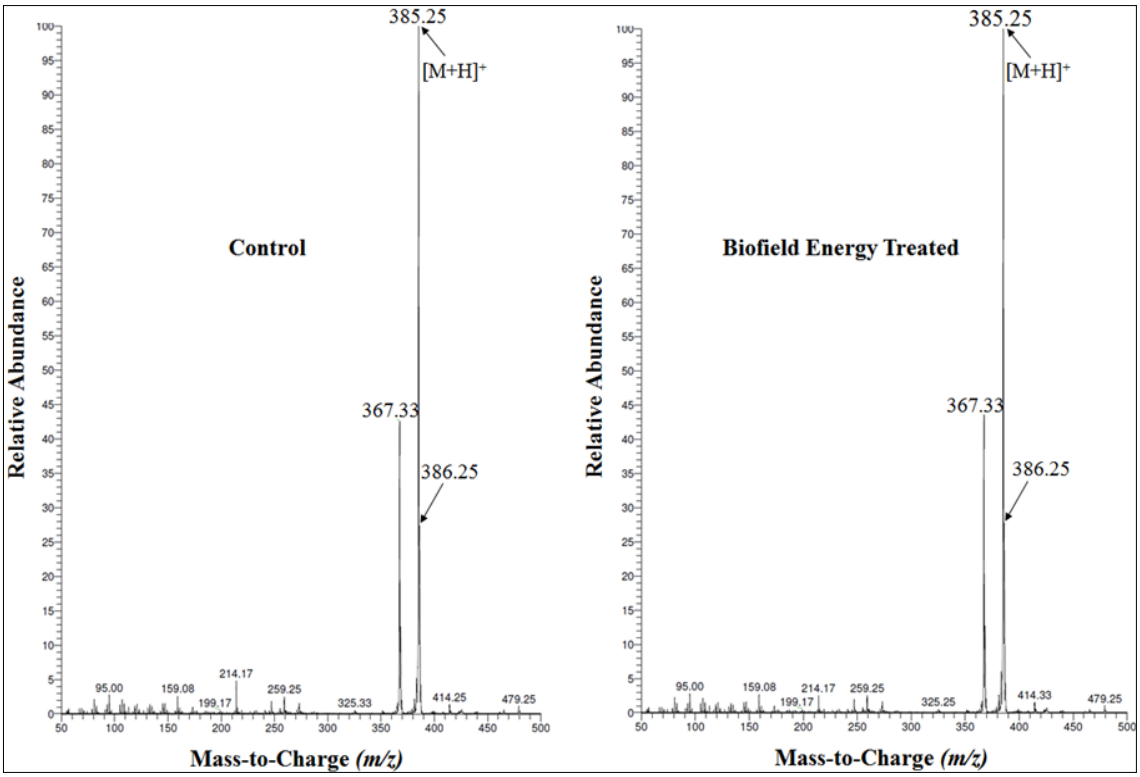

Figure 2. Mass spectra of the control and Biofield Energy Treated cholecalciferol.

(Figures 2 and 3). The experimental data were well matched with the literature data [39].

The cholecalciferol samples showed the mass of a molecular ion at *m/z* 385.25 (calcd for $C_{27}H_{45}O^+$, 385.35) with 100% relative abundance in the spectra. The theoretical calculation of isotopic peak P_{M+1} for the protonated cholecalciferol presented as below:

P (^{13}C) = [(27 x 1.1%) x 100% (the actual size of the M^+ peak)] / 100% = 29.7%

P (^{2}H) = [(45 x 0.015%) x 100%] / 100%= 0.675%

P (^{17}O) = [(1 x 0.04%) x 100%] / 100% = 0.04%

P_{M+1} *i. e.* ^{13}C, ^{2}H, and ^{17}O contributions from $C_{27}H_{45}O^+$ to *m/z* 386.25 = 30.42%

The calculated isotopic abundance of P_{M+1} value 30.42% was higher to the experimental value (27.21%) (Table 1). From the above calculation, it has been found that ^{13}C has the major contribution to *m/z* 386.25.

The LC-MS based isotopic abundance ratio analysis P_M and P_{M+1} for cholecalciferol near *m/z* 385.25 and 386.25, respectively, which were obtained from the observed relative peak intensities of $[M^+]$ and $[(M+1)^+]$ peaks, respectively in the ESI-MS spectra (Table 1). The isotopic abundance ratio of P_{M+1}/P_M ($^{2}H/^{1}H$ or $^{13}C/^{12}C$ or $^{17}O/^{16}O$) in treated cholecalciferol was increased by 0.74% compared to the control sample (Table 1). Thus, the ^{13}C, ^{2}H, and ^{17}O contributions from $C_{27}H_{45}O^+$ to *m/z* 386.25 in the treated cholecalciferol was increased compared to the control sample.

Gas Chromatography-Mass Spectrometry (GC-MS) Analysis

The cholecalciferol samples showed two major independent peaks in the GC-MS chromatograms (Figure 3). The R_t of the control cholecalciferol was at 22.06 and 22.74 minutes, whereas 21.95 and 22.62 minutes is for the treated cholecalciferol, which indicated that the polarity of both the sample was very close. The two peaks in the chromatograms of both the cholecalciferol samples might be due to the cis and trans isomers of cholecalciferol [40, 41].

The GC-MS spectra of the cholecalciferol samples at R_t of 22 minutes exhibited the presence of the molecular ion peak of cholecalciferol ($C_{27}H_{44}O^+$) (Figure 4) at *m/z* 385 (calcd for $C_{27}H_{44}O^+$, 384.34). The low molecular mass fragmentation peak at *m/z* 367, and 352 for $C_{27}H_{43}^+$ and $C_{26}H_{40}^+$, respectively were also observed in both the spectra (Figure 4). The mass peak intensities of the Biofield Energy Treated cholecalciferol were altered compared to the control sample.

The GC-MS spectra of both the cholecalciferol showed the mass of the molecular ion peak $[M]^+$ at *m/z* 385 (calcd for $C_{27}H_{44}O^+$, 384.34). The theoretical calculation of P_{M+1} and P_{M+2} for cholecalciferol was presented as below:

P (^{13}C) = [(27 x 1.1%) x 10% (the actual size of the M^+ peak)] / 100% = 2.97%

P (^{2}H) = [(44 x 0.015%) x 10%] / 100%= 0.07%

P (^{17}O) = [(1 x 0.04%) x 10%] / 100% = 0.004%

P_{M+1} *i. e.* ^{13}C, ^{2}H, and ^{17}O contributions from $C_{27}H_{45}O^+$ to *m/z* 386 = 3.04%

Similarly, the theoretical calculation of isotopic peak P_{M+2} for the protonated cholecalciferol was presented below:

P (^{18}O) = [(1 x 0.20%) x 10%] / 100% = 0.02%

P_{M+2} of ^{18}O contribution from $C_{27}H_{45}O^+$ to *m/z* 387 = 0.02%

The calculated isotopic abundance of P_{M+1} and P_{M+2} values were close to the calculated value (Table 2). From the above calculation, it has been found that ^{13}C and ^{18}O have major contribution to *m/z* 386 and 387 of cholecalciferol.

The GC-MS based isotopic abundance ratio analysis of the treated sample was calculated compared to the control sample. P_M, P_{M+1}, and P_{M+2} for cholecalciferol near *m/z* 385, 386, and 387, respectively of the control and treated samples, which were obtained from the observed relative peak intensities of $[M^+]$, $[(M+1)^+]$, and $[(M+2)^+]$ peaks, respectively in the mass spectra. The isotopic abundance ratio of P_{M+1}/P_M and P_{M+2}/P_M in the treated cholecalciferol was significantly increased by 66.39% and 62.69%, respectively compared to the control sample (Table 2). Therefore, the ^{13}C, ^{2}H, ^{17}O and ^{18}O contributions from $C_{27}H_{44}O^+$ to *m/z* 386 and 387 in the treated cholecalciferol were significantly increased compared with the control sample. Fig 5.

LC-MS and GC-MS study confirmed the

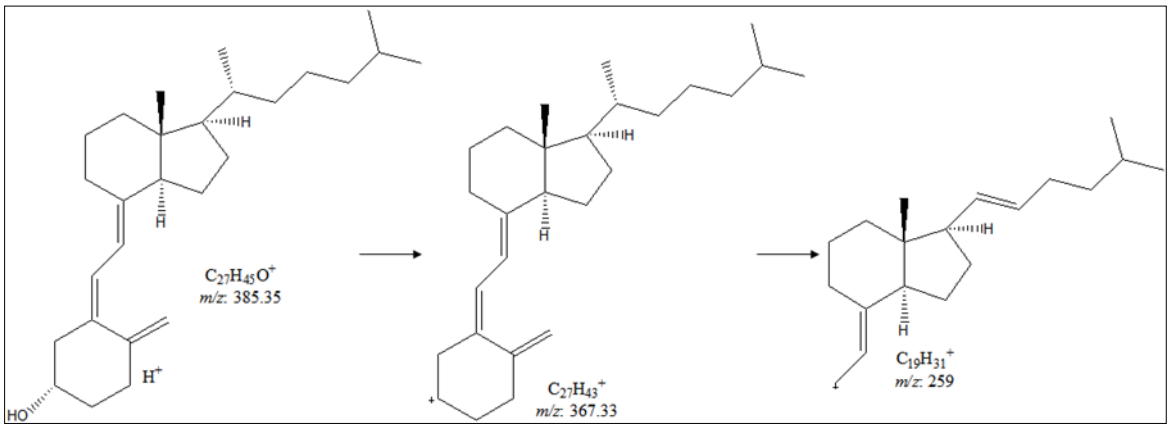

Figure 3. Proposed fragmentation pattern of cholecalciferol.

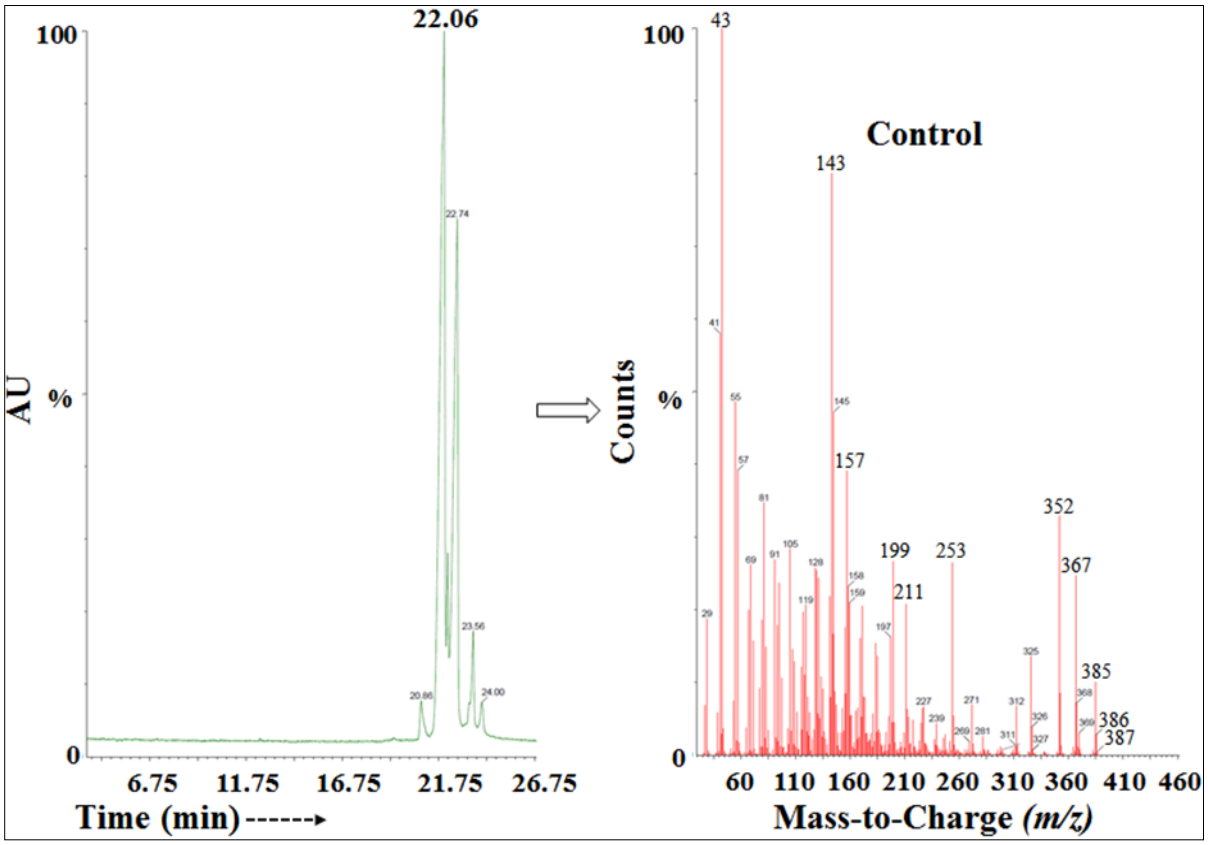

Figure 4. The GC-MS chromatogram and mass spectra of the control cholecalciferol.

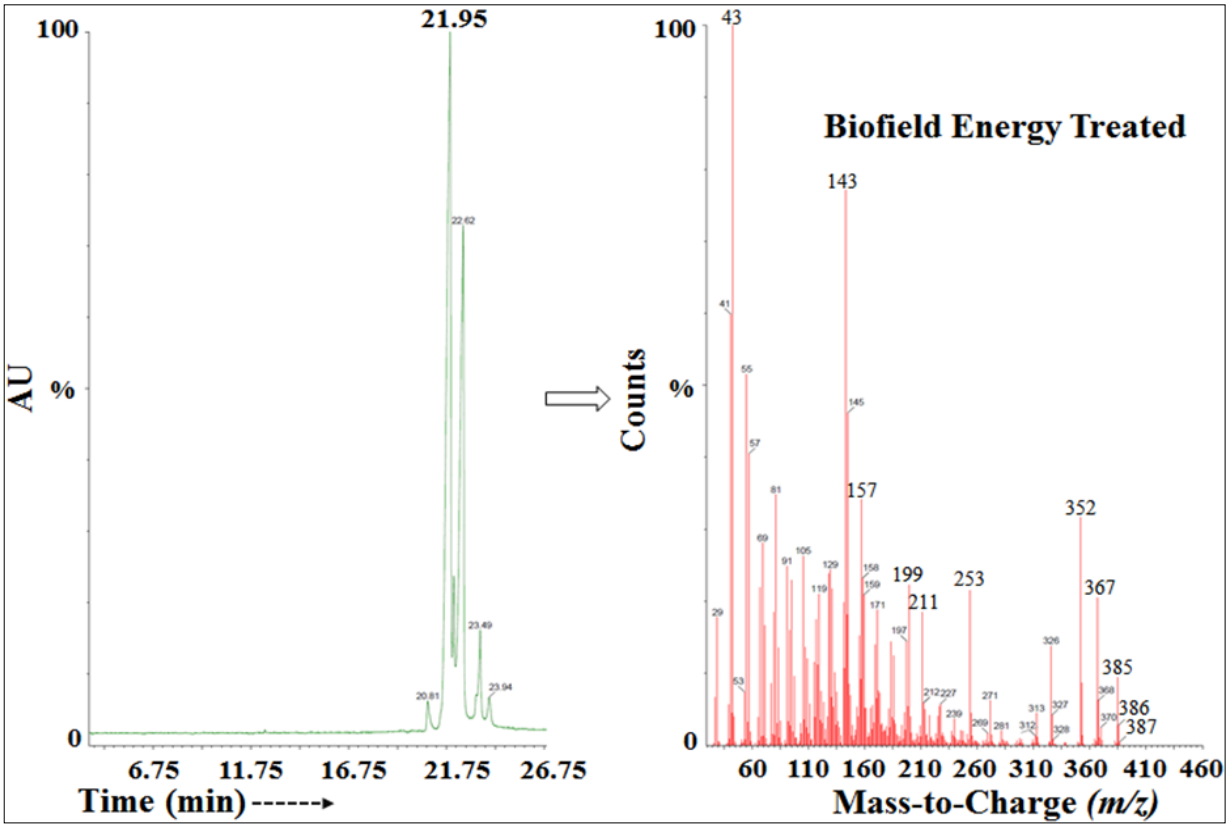

Figure 5. The GC-MS chromatogram and mass spectra of the Biofield Energy Treated cholecalciferol.

Table 1. LC-MS based isotopic abundance analysis results in Biofield Energy Treated cholecalciferol compared to the control sample.

Parameter	Control Sample	Biofield Energy Treated Sample
P_M at *m/z* 385.25 (%)	100	100
P_{M+1} at *m/z* 386.25 (%)	27.21	27.41
P_{M+1}/P_M	0.27	0.27
% Change of isotopic abundance ratio (P_{M+1}/P_M) with respect to the control sample		0.74

P_M: the relative peak intensity of the parent molecular ion [M^+]; P_{M+1}: the relative peak intensity of the isotopic molecular ion [$(M+1)^+$], M: mass of the parent molecule.

Table 2. GC-MS based isotopic abundance analysis results of Biofield Energy Treated cholecalciferol compared to the control samples.

Parameter	Control Sample	Biofield Energy Treated Sample
P_M at *m/z* 385 (%)	10.00	6.01
P_{M+1} at *m/z* 386 (%)	2.77	2.77
P_{M+1}/P_M	0.28	0.46
% Change of isotopic abundance ratio (P_{M+1}/P_M) compared to the control sample		66.39
P_{M+2} at *m/z* 387 (%)	0.45	0.44
P_{M+2}/P_M	0.05	0.07
% Change of isotopic abundance ratio (P_{M+2}/P_M) compared to the control sample		62.69

P_M: the relative peak intensity of the parent molecular ion [M^+]; P_{M+1}: the relative peak intensity of the isotopic molecular ion [$(M+1)^+$]; P_{M+2}: the relative peak intensity of the isotopic molecular ion [$(M+2)^+$]; M: mass of the parent molecule.

structure of cholecalciferol. The isotopic abundance ratios of P_{M+1}/P_M ($^2H/^1H$ or $^{13}C/^{12}C$ or $^{17}O/^{16}O$) and P_{M+2}/P_M ($^{18}O/^{16}O$) in the treated cholecalciferol were significantly increased compared to the control sample. The altered isotopic composition of the Trivedi Effect®-Consciousness Energy Healing Treated cholecalciferol might have altered the neutron to proton ratio in the nucleus *via* the possible mediation of neutrino [15]. Neutrino is a subatomic particle but has no electrical charge and a very small mass. These are one of the most abundant particles in the universe. The neutrinos have the ability to interact with protons and neutrons in the nucleus, which might have a close relation between neutrino and the isotope formation [15, 34, 35]. The isotopic abundance ratios $^2H/^1H$ or $^{13}C/^{12}C$ or $^{17}O/^{16}O$ or $^{18}O/^{16}O$ would influence the atomic bond vibration of treated cholecalciferol [42]. The increased isotopic abundance ratio of the treated cholecalciferol may increase the intra-atomic bond strength, increase its stability. The Biofield Energy Treated cholecalciferol would be more stable and suitable for the prevention and treatment of various diseases such as vitamin D deficiency, rickets, osteoporosis, arthritis, multiple sclerosis, cancer, diabetes mellitus, mental disorders, cardiovascular diseases, hypertension, infections, influenza, cognitive impairment in older adults, Parkinson's and Alzheimer's diseases, autoimmune disease, dementia, glucose intolerance, multiple sclerosis, etc.

Conclusions

The Trivedi Effect®-Consciousness Energy Healing Treatment has shown a significant impact on the isotopic abundance ratios of cholecalciferol. The LC-MS spectra of both the samples at retention time (R_t) ~22 minutes exhibited the mass of the molecular ion peak at *m/z* 385.25. The LC-MS based isotopic abundance ratio of P_{M+1}/P_M in the Biofield Energy Treated cholecalciferol was increased by 0.74% compared with the control sample. But, the GC-MS based isotopic abundance ratio of P_{M+1}/P_M and P_{M+2}/P_M in the Biofield Energy Treated cholecalciferol was

significantly increased by 66.39% and 62.69%, respectively compared with the control sample. Hence, ^{13}C, ^{2}H, ^{17}O and ^{18}O contributions from $C_{27}H_{44}O^{+}$ to *m/z* 386 and 387 in the Biofield Energy Treated cholecalciferol were significantly increased compared with the control sample. The isotopic abundance ratios of P_{M+1}/P_M ($^{2}H/^{1}H$ or $^{13}C/^{12}C$ or $^{17}O/^{16}O$) and P_{M+2}/P_M ($^{18}O/^{16}O$) in the treated cholecalciferol were significantly increased compared to the control sample. The increased isotopic composition of the Trivedi Effect®-Consciousness Energy Healing Treated cholecalciferol might have altered the neutron to proton ratio in the nucleus *via* the possible mediation of neutrino. The increased isotopic abundance ratio of the Biofield Energy Treated cholecalciferol may increase the intra-atomic bond strength, increase its stability. The new form of cholecalciferol would be better designing novel pharmaceutical formulations that might be more stable and more efficacious for the prevention and treatment of various diseases *viz.* rickets, osteoporosis, arthritis, multiple sclerosis, cancer, diabetes mellitus, mental disorders, cardiovascular diseases, hypertension, infections, influenza, cognitive impairment in older adults, Parkinson's and Alzheimer's diseases, autoimmune disease, dementia, glucose intolerance, multiple sclerosis, etc.

Acknowledgements

The authors are grateful to Sophisticated Instrumentation Centre for Applied Research & Testing (SICART) India, Trivedi Science, Trivedi Global, Inc., and Trivedi Master Wellness for their assistance and support during this work.

References

1. Kulie T, Groff A, Redmer J, Hounshell J, Schrager S (2009) Vitamin D: An evidence-based review. J Am Board Fam Med 22: 698-706.
2. Nair R, Maseeh A (2012) Vitamin D: The "sunshine" vitamin. J Pharmacol Pharmacother 3: 118-26.
3. Coulston AM, Carol B, Mario F (2013) Nutrition in the prevention and treatment of disease. Academic Press. p 818.
4. Samuel S, Sitrin MD (2008) Vitamin D's role in cell proliferation and differentiation. Nutr Rev 66: S116-124.
5. Simana E, Simian R, Portnoy S, Jaffe, A, Dekel BZ (2015) Feasibility Study -Vitamin D loading determination by FTIR-ATR. Information & Control Systems76: 107-111.
6. Ritu G, Gupta A (2014) Vitamin D deficiency in India: Prevalence, causalities and interventions. Nutrients 6: 729-775.
7. Lawson DE, Wilson PW, Kodicek E. (1969) Metabolism of vitamin D. A new cholecalciferol metabolite, involving loss of hydrogen at C-1, in chick intestinal nuclei. Biochem J 115: 269-277.
8. Ross CA, Taylor CL, Yaktine AL, Valle HBD (2010) Dietary reference intakes for calcium and Vitamin D. Washington (DC): National Academies Press (US); 2011. (access on 02.05.2018)
9. Koshy KT, Beyer WF (1984) Vitamin D_3 (Cholecalciferol) in analytical profiles of drug substances, Florey K (Ed.), Vol 13, Academic Press, Inc., Orlando, USA, pp. 656-707.
10. Collins ED, Norman AW (2001) Vitamin D in Handbook of Vitamins, 3rd Edn., Rucker RB, Suttie JW, McCormick DB, Machlin LJ, Marcel Dekker, Inc., New York, pp. 51-114.
11. Lehmann U, Hirche F, Stangl GI, Hinz K, Westphal S, Dierkes J (2013) Bioavailability of vitamin D(2) and D(3) in healthy volunteers, a randomized placebo-controlled trial. J Clin Endocrinol Metab 98: 4339-4345.
12. Branton A, Jana S (2017) The influence of energy of consciousness healing treatment on low bioavailable resveratrol in male Sprague Dawley rats. International Journal of Clinical and Developmental Anatomy 3: 9-15.
13. Branton A, Jana S (2017) The use of novel and unique biofield energy healing treatment for the improvement of poorly bioavailable compound, berberine in male Sprague Dawley rats. American Journal of Clinical and Experimental Medicine 5: 138-144.
14. Branton A, Jana S (2017) Effect of The biofield energy healing treatment on the pharmacokinetics of 25-hydroxyvitamin D_3 [25(OH)D_3] in rats after a single oral dose of vitamin D_3. American Journal of

Pharmacology and Phytotherapy 2: 11-18.

15. Trivedi MK, Mohan TRR (2016) Biofield energy signals, energy transmission and neutrinos. American Journal of Modern Physics 5: 172-176.
16. Rubik B, Muehsam D, Hammerschlag R, Jain S (2015) Biofield science and healing: history, terminology, and concepts. Global Advances in Health and Medicine 4: 8-14.
17. Warber SL, Cornelio D, Straughn, J, Kile G (2004) Biofield energy healing from the inside. J Altern Complement Med 10: 1107-1113.
18. Movaffaghi Z, Farsi M (2009) Biofield therapies: Biophysical basis and biological regulations? Complement Ther Clin Pr 15: 35-37.
19. Koithan M (2009) Introducing complementary and alternative therapies. J Nurse Pract 5: 18-20.
20. Barnes PM, Bloom B, Nahin RL (2008) Complementary and alternative medicine use among adults and children: United States, 2007. Natl Health Stat Report 12: 1-23.
21. Dabhade VV, Tallapragada RMR, Trivedi MK (2009) Effect of external energy on the atomic, crystalline, and powder characteristics of antimony and bismuth powders. Bulletin of Materials Science 32: 471-479.
22. Trivedi MK, Patil S, Tallapragada RM Effect of biofield treatment on the physical and thermal characteristics of Silicon, Tin and Lead powders. J Material Sci Eng 2:125.
23. Nayak G, Trivedi MK, Branton A, Trivedi D, Jana S (2018) The physicochemical and thermal properties of consciousness energy healing treated silver oxide (Ag_2O). Aspects in Mining & Mineral Science. 2: 1-6.
24. Nayak G, Trivedi MK, Branton A, Trivedi D, Jana S (2018) Evaluation of the physicochemical and thermal properties of chromium trioxide (CrO3): Impact of consciousness energy healing treatment. Research & Development in Material Science. 8: 1-6.
25. Trivedi MK, Branton A, Trivedi D, Nayak G, Sethi KK, Jana S (2016) Determination of isotopic abundance ratio of biofield energy treated 1,4-dichlorobenzene using gas chromatography-mass spectrometry (GC-MS). Modern Chemistry 4: 30-37.
26. Trivedi MK, Branton A, Trivedi D, Nayak G, Panda P, Jana S (2016) Gas chromatography-mass spectrometric analysis of isotopic abundance of ^{13}C, ^{2}H, and ^{18}O in biofield energy treated p-tertiary butylphenol (PTBP). American Journal of Chemical Engineering 4: 78-86.
27. Trivedi MK, Branton A, Trivedi D, Nayak G, Mondal SC, Jana S (2015) Antimicrobial sensitivity, biochemical characteristics and biotyping of *Staphylococcus saprophyticus*: An impact of biofield energy treatment. J Women's Health Care 4: 271.
28. Trivedi MK, Branton A, Trivedi D, Nayak G, Shettigar H, Gangwar M, Jana S (2015) Antibiogram of multidrug-resistant isolates of *Pseudomonas aeruginosa* after biofield treatment. J Infect Dis Ther 3: 244.
29. Trivedi MK, Branton A, Trivedi D, Nayak G, Gangwar M, Jana S (2015) Agronomic characteristics, growth analysis, and yield response of biofield treated mustard, cowpea, horse gram, and groundnuts. International Journal of Genetics and Genomics. 3: 74-80.
30. Sances F, Flora E, Patil S, Spence A, Shinde V (2013) Impact of biofield treatment on ginseng and organic blueberry yield. AGRIVITA, Journal of Agricultural Science 35: 1991-8178.
31. Trivedi MK, Branton A, Trivedi D, Nayak G, Sethi KK, Jana S (2016) Isotopic abundance ratio analysis of biofield energy treated indole using gas chromatography-mass spectrometry. Science Journal of Chemistry 4: 41-48.
32. Trivedi MK, Branton A, Trivedi D, Nayak G, Panda P, Jana S (2016) Evaluation of the isotopic abundance ratio in biofield energy treated resorcinol using gas chromatography-mass spectrometry technique. Pharm Anal Acta 7: 481.
33. Schellekens RC, Stellaard F, Woerdenbag HJ, Frijlink HW, Kosterink JG (2011) Applications of stable isotopes in clinical pharmacology. Br J Clin Pharmacol 72: 879-897.
34. Muccio Z, Jackson GP (2009) Isotope ratio mass spectrometry. Analyst 134: 213-222.
35. Weisel CP, Park S, Pyo H, Mohan K, Witz G (2003)

Use of stable isotopically labeled benzene to evaluate environmental exposures. J Expo Anal Environ Epidemiol 13: 393-402.

36. Rosman KJR, Taylor PDP (1998) Isotopic compositions of the elements 1997 (Technical Report). Pure Appl Chem 70: 217-235.
37. Smith RM (2004) Understanding Mass Spectra: A Basic Approach, Second Edition, John Wiley & Sons, Inc.
38. Jürgen H (2004) Gross Mass Spectrometry: A Textbook (2nd Edn) Springer: Berlin.
39. https://www.drugbank.ca/spectra/ms_ms/61218. Retrieved on 02 May 2018.
40. Holick MF, Garabedian M, DeLuca HF (1972) 5,6-Trans isomers of cholecalciferol and 25-hydroxycholecalciferol. Substitutes for 1, 25-dihydroxycholecalciferol in anephric animals. Biochemistry 11: 2715–2719.
41. Okamura WH, Midland MM, Hammond MW, Abd Rahman N, Dormanen MC, Nemere I, Norman AW (1995) Chemistry and conformation of vitamin D molecules. J Steroid Biochem Mol Biol 53: 603-613.
42. Santesteban LG, Miranda C, Barbarin I, Royo JB (2014) Application of the measurement of the natural abundance of stable isotopes in viticulture: A review. Australian Journal of Grape and Wine Research 21: 157-167.